*Journal of Experimental Zoology Part A: Ecological and Integrative Physiology*

WILEY

JEZ-A ECOLOGICAL AND INTEGRATIVE PHYSIOLOGY

RESEARCH ARTICLE OPEN ACCESS

# Influence of Habitat Use on Prey Capture Behavior and Kinematics in the Pyrenean Brook Newt (*Calotriton asper*)

Noah Heier[1] | Isabelle Toussaint-Lardé[1,2,3] | Olivier Guillaume[4] | Anthony Herrel[1,2,5,6] | Anne-Claire Fabre[2,3,7]

[1]Mécanismes Adaptatifs et Evolution, UMR 7179, Muséum national d'Histoire naturelle CNRS, Paris, France | [2]Naturhistorisches Museum der Burgergemeinde Bern, Bern, Switzerland | [3]Institute of Ecology & Evolution, Universität Bern, Bern, Switzerland | [4]Station d'Ecologie Théorique et Expérimentale (SETE), UAR2029 Centre National de la Recherche Scientifique (CNRS), Moulis, France | [5]Department of Biology, Evolutionary Morphology of Vertebrates, Ghent University, Ghent, Belgium | [6]Department of Biology, University of Antwerp, Wilrijk, Belgium | [7]Department of Life Sciences, Natural History Museum, London, UK

**Correspondence:** Isabelle Toussaint-Lardé (isabelle.toussaint@students.unibe.ch)

**Received:** 4 May 2026 | **Revised:** 22 July 2026 | **Accepted:** 28 August 2026

**Funding:** European Research Council Starting Grant, Grant/Award Number: M822.00039

**Keywords:** behavior | cave | feeding | kinematics | sensory system | urodela

## ABSTRACT

Caves are extreme environments that impose stringent selective pressures on organisms. Consequently, many cave dwellers show extreme adaptations such as the loss of eyes, depigmentation, and a low resting metabolic rate. Yet, how the initial stages of adaptation to these extreme environments take place remains poorly understood. *Calotriton asper* is a species of salamander that is ideal to understand the initial stages of adaptation to underground environments. This species presents two genetically distinct morphotypes that live either in surface streams or in cave streams, yet without showing obvious morphological differences. Here, we test for differences in the capacity to locate prey and differences in feeding kinematics between cave-dwelling and surface-dwelling populations under different light conditions. To do so, we quantified prey location ability using a Y-maze and filmed animals capturing prey using high-speed video cameras, both in light and in full darkness. Our results show that animals change capture style and exploration behavior in function of light conditions suggesting an intrinsic plasticity in the species allowing it to feed in both environments. However, the kinematics of capture suggest population-specific behaviors allowing cave-dwellers to be more efficient in capturing prey under total darkness.

## 1 | Introduction

The availability of trophic resources is a major factor driving the evolution of feeding structures and their function (Schwenk 2000; Herrel et al. 2019). For example, Darwin's finches show variation in beak and head shape allowing them to efficiently use different resources (Grant and Grant 2005; Herrel et al. 2005a, 2005b; Soons et al. 2010, 2015). Extreme environments, such as arid regions, small islands, polar areas, rocky coasts, and deep-sea aphotic zones, impose significant challenges due to temperature extremes, mechanical forces, and physicochemical constraints like salinity, dryness, and lack of light. These conditions often limit resource availability, creating additional selective pressures. These selective pressures push species to adapt and explore novel resources, especially when resources are scarce (Herrel et al. 2008; Castilla et al. 2011). Despite these challenges, many species have adapted to thrive in such extreme environments, demonstrating remarkable evolutionary adaptations.

Noah Heier and Isabelle Toussaint-Lardé are co-first authors. Anthony Herrel and Anne-Claire Fabre are co-last authors.

**Research Highlights**

- Surface and cave *Calotriton asper* detect food equally well, using both vision and olfaction.
- "Ram" compensatory-suction strikes dominate in the light, while "static" inertial suction dominates in darkness.
- Both populations shift toward the other's behavior when light conditions are switched.
- Yet this shift lacks the finer kinematic tuning of the native population, hinting at incipient local adaptation.
- Switching an animal to the other population's condition induces that population's behavior, but without its full kinematic subtleties.

Caves represent a unique environment characterized by the absence of light, high humidity, and limited resources (Poulson and White 1969; Culver and Pipan 2009). These factors make energy acquisition a primary driver of evolution in caves. Cave ecosystems are typically supported by two types of food chains: detritus-based and chemo-litho-autotrophic bacteria-based (Venarsky and Huntsman 2018). Species in these environments exhibit specializations such as slow life cycles and metabolic rates (Moran et al. 2014; Hervant et al. 2000), depigmentation, and eye loss (Cartwright et al. 2017), as well as enhanced olfactory and tactile senses (Soares and Niemiller 2020). For instance, the olm (*Proteus anguinus*), a blind, depigmented, and neotenic salamander, has a highly developed olfactory sense, capable of detecting prey at small concentrations in water currents (Dumas and Chris 1998). These salamanders also exhibit exceptional longevity (65 years on average) and lack circadian rhythms, with a slow metabolism and low activity levels in response to the limited resource availability (Voituron et al. 2010; Hervant et al. 2000). Interestingly, many salamanders have independently radiated into cave environments making them a perfect group to understand adaptation to life in the dark (Phillips et al. 2017).

The Pyrenean brook newt, *Calotriton asper*, provides an excellent model for studying evolutionary adaptations to cave environments. These largely aquatic newts are endemic to the Pyrenean mountains, inhabiting altitudes from 100 to 2500 m (Talavera et al. 2023). Populations are divided between surface streams and subterranean waters (cave-dwelling). These populations are highly isolated, with minimal gene flow between them (Valbuena-Ureña et al. 2018). Cave colonization occurred relatively recently, about 10,000 years ago (Issartel et al. 2010). Despite living in caves, cave-dwelling populations do not display the extreme traits of obligate cave dwellers (Guillaume et al. 2020; Hervant et al. 2001). Consequently, comparing cave and surface-dwelling populations of this species can shed light on the initial stages of adaptation to cave environments. Due to the lack of light and resources, both the ability to locate and the ability to capture prey are likely under strong selection. Cave-dwelling salamanders typically adopt an active foraging strategy (Uiblein et al. 1992; Manenti et al. 2020). However, whereas most surface-active salamanders use visual cues to locate and capture prey (Borghuis and Leonardo 2015) cave-dwelling salamanders such as the olm (*Proteus anguinus*) use mechanical and chemical cues. Previous studies have demonstrated that facultative cave-dwellers like *Calotriton asper* use predominantly visual cues under light conditions but switch to an active widely foraging strategy when feeding in darkness (Uiblein et al. 1992).

Surface-dwelling salamanders have access to a larger number of prey including insects, other invertebrates, and larvae found both on land and in small rivers or lakes (Sánchez-Hernández et al. 2019). In contrast, cave-dwelling salamanders have a more restricted diet, as caves typically harbor a lower diversity and abundance of arthropods (Gibert and Deharveng 2002). However, their diet remains similar, consisting mainly of small insects and invertebrate larvae. Under water salamanders typically use suction feeding. This method involves a rapid expansion of the buccal cavity, creating a water flow that draws in prey (Deban 2003; Larsen and Guthrie 1975). The mechanics of suction feeding involve coordinated jaw and hyobranchial movements to generate effective suction, crucial for capturing prey in water (Lauder and Shaffer 1986). However, suction feeding is only effective right in front of the mouth and fluid velocity declines rapidly with the distance from the mouth (Day et al. 2005). Two types of suction feeding have been described previously: inertial suction where the animal remains immobile while the prey is drawn into the mouth, or compensatory suction where the animal lunges forward and the hyoid depression serves to offset the water pushed in front of the animal, this preventing the prey from being displaced (Van Damme and Aerts 1997). In dark caves, salamanders should approach the prey more closely to ensure effective capture as the chances of finding the prey again after escape are low. Moreover, feeding near a substrate has been shown to extend the diameter over which suction is effective (Nauwelaerts et al. 2007) suggesting that cave-dwelling salamanders should try to take advantage of this mechanism. Yet, whether cave-dwelling salamanders do so and have adapted the kinematics of suction feeding remains unknown.

Here, we test individuals from both cave- and surface-dwelling populations in light and full darkness to explore whether prey location and capture strategies are flexible or dependent on the environment of origin. We hypothesize that animals from cave environments will be more efficient at locating prey in total darkness and that their feeding kinematics will allow them to efficiently capture prey in total darkness by moving closer to the prey and relying principally on inertial suction. Conversely, we predict that surface-dwelling populations should show greater behavioral flexibility allowing them to potentially explore both environments.

## 2 | Materials and Methods

### 2.1 | Animals

*Calotriton asper* were maintained in the Moulis cave which is part of the Theoretical and Experimental Ecology Station (SETE) in the Pyrenean mountains, France. Individuals were captured in caves or in surface rivers about 5–6 years prior to this study and have since been maintained under experimental conditions in this cave. None of the individuals used were born

and raised in the facility. The salamanders were kept under the light conditions corresponding to their environment of origin either under 12 h light-dark cycles (surface dwelling populations) or in total darkness (cave populations). Animals from surface populations were kept in glass aquaria with a continuous water flow from the cave ($10.13 \pm 0.19$ ppm $O_2$, $9.90 \pm 0.21$°C; Guillaume et al. 2020), in a room with a 12-h light/dark cycle simulating natural conditions. Cave animals were housed in similar aquaria but in a constantly dark area of the cave. Oxygen concentration and temperature were monitored using FireSting fiber optic oxygen detectors (PyroScience). We used ten individuals for each experiment, five surface-dwelling and five cave-dwelling. Different individuals were used to obtain a robust, independent sample for each test. Body length and body mass are reported in Tables S2 and S3. No significant differences were detected between the groups of origin for the olfactory/exploratory behavior experiments (body mass: 8.04 vs. 8.25 g; Student's *t*-test, $p = 0.85$) or the feeding kinematics experiments (body length: 7.12 vs. 7.26 cm; Student's *t*-test, $p = 0.43$). We used only females to avoid potential sexual differences in behavior or kinematics. For both experiments, each animal was tested under two light conditions: light or dark. Four conditions were thus tested: surface-dwelling individuals in light conditions, surface-dwelling individuals in total darkness, cave-dwelling individuals in total darkness, and cave-dwelling individuals in light conditions (Tables S1–S3).

## 2.2 | Y-Maze Trials

The Y maze was a round open field, 70 cm in diameter with two 25 cm long, 10 cm diameter tunnels positioned at a 45° angle from each other (Figure 1A). Light conditions consisted either of overhead electric lights and infrared light or only infrared light, outside the visual range of salamanders and therefore likely not detectable by *Calotriton asper* (Dedolight DLED2Y 20 W infrared 860 nm LED lights). A Sony Handycam with a nightshot option was placed to record the upper half of the open field and the two tunnels. At the end of the tunnels, a rock, or a tea bag full of blood worms, was placed. The rock, roughly the same size and shape as the filled tea bag, was used as a visual element to account for potential shelter preferences and to ensure that the choice was based on food detection only. A few additional free-ranging blood worms were added to the end of the tunnel with the food. The placement of the food was randomized between the left and the right tunnel. The maze was filled with water from the cave and individuals were placed at the furthest point from the two tunnels, at the far end of the maze. Animals were recorded for 15 min. Each individual was filmed twice a day for 10 consecutive days (with 5 h between observations) to obtain 10 videos per individual for each light condition (a total of 200 videos). We alternated the light conditions each day. Videos were manually analyzed by splitting the maze in 5 sectors: the lower half, the top right quadrant, the top left quadrant, the right tunnel, and the left tunnel. For each video, the time of first entry into a tunnel was recorded as well as the time spent in each sector. The individual was considered to enter a new sector when its head had fully entered it. See Table S2 for raw value and Table 1 for means and standard deviations of the variables.

## 2.3 | High-Speed Video Recordings of Prey Capture

We use a high-speed video camera (Phantom Miro R 311; 1280 by 800 pixel resolution) recording at 700 or 1000 frames

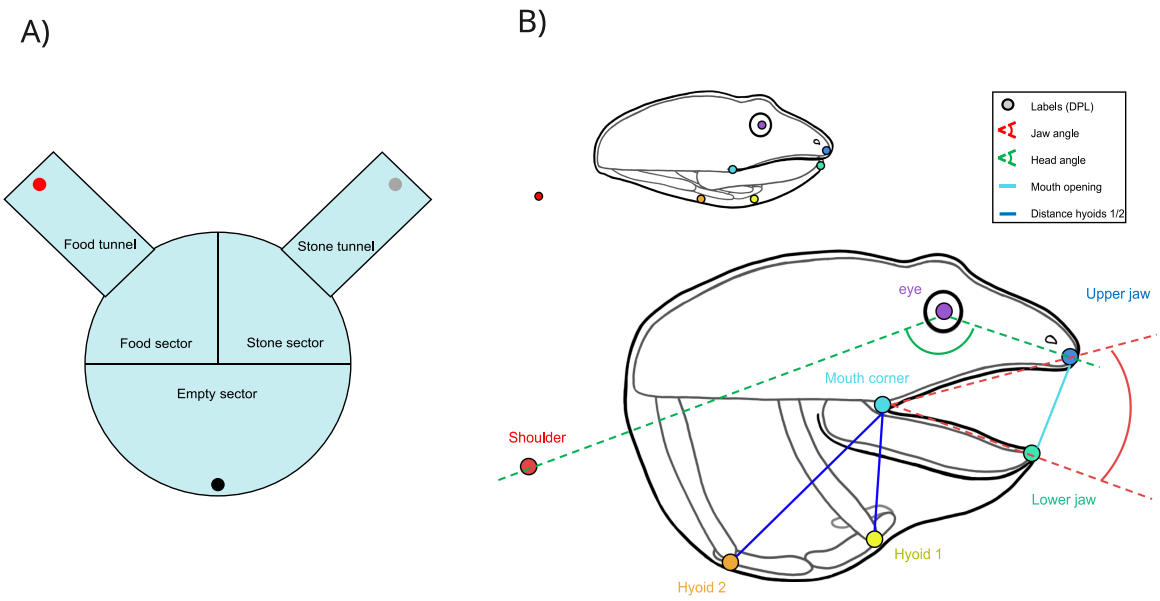


**FIGURE 1** | (A) Experimental set-up used for olfaction and exploration tests. Schematic representation of the Y-maze used for recording videos of *Calotriton asper* exploring their environment under light and dark conditions. In the light treatment, both light sources (white light and infrared) are used, while in conditions of total darkness only infrared lights are present. The maze is an open-topped cylindrical structure filled with water, divided into five main sectors: the food sector, the stone sector, and an empty sector. The red circle represents the location of the food source; the gray circle represents the location of the rock. The black circle indicates the initial position of the individual before exploration begins. The placement of the food and stone is randomized between trials. (B) Schematic representation of landmarks used and kinematic variables extracted.

**TABLE 1** | Means and standard deviations of the behavioral parameters extracted from the maze trials.

| Origin<br>Light Condition | Surface<br>Light | Surface<br>Dark | Cave<br>Light | Cave<br>Dark |
|---|---|---|---|---|
| Time first entry (s) | 297.2 ± 130.92 | 420.64 ± 181.47 | 366.4 ± 158.26 | 351.4 ± 187.11 |
| Time entry correct tunnel (s) | 321.72 ± 170.53 | 310.9 ± 229.54 | 350.44 ± 199.08 | 285.82 ± 239.32 |
| Time in food sector (s) | 320.86 ± 96.34 | 360.52 ± 185.82 | 387.4 ± 146.07 | 380.46 ± 176.12 |
| Time in food tunnel (s) | 152.92 ± 88.60 | 205 ± 179.44 | 220.22 ± 154.99 | 179.62 ± 161.12 |
| Time in food sector (%) | 35.65 ± 10.7 | 40.05 ± 20.65 | 43.04 ± 16.23 | 42.27 ± 19.6 |
| Time in food tunnel (%) | 16.99 ± 9.84 | 22.78 ± 19.94 | 24.47 ± 17.22 | 19.96 ± 17.90 |
| Time in stone sector (s) | 257.8 ± 82.06 | 159.48 ± 109.87 | 207.3 ± 111.64 | 197.66 ± 107.91 |
| Time in stone tunnel (s) | 105.7 ± 84.172 | 60.6 ± 86.49 | 74.18 ± 90.44 | 66.16 ± 76.31 |
| Time in stone sector (%) | 28.64 ± 9.12 | 17.72 ± 12.21 | 23.03 ± 12.40 | 21.96 ± 11.99 |
| Time in stone tunnel (%) | 11.74 ± 9.35 | 6.73 ± 9.61 | 8.24 ± 10.05 | 7.35 ± 8.48 |
| Time in empty sector (%) | 35.7 ± 7.05 | 42.22 ± 13.51 | 33.92 ± 10.32 | 35.76 ± 11.48 |
| Number of entries in food tunnel | 1.44 ± 0.75 | 0.78 ± 0.56 | 1.18 ± 0.61 | 0.92 ± 0.59 |
| Number of entries in the stone tunnel | 1.26 ± 0.91 | 0.36 ± 0.49 | 0.62 ± 0.67 | 0.58 ± 0.70 |

per second to quantify prey capture kinematics. Animals were transferred to a filming tank with water from the cave. The camera was positioned in lateral view with a 1 cm grid in the background used for scaling. Bloodworms were manually introduced into the tank within the camera's field of view. Animals were filmed under the same two light conditions as the previous experiment, either illuminated with overhead electric lights and infrared lights or in full darkness, illuminated only by infrared light. The high-speed camera was connected to a computer running the Phantom Camera Control software (V. 3.8). A total of 182 videos were recorded, with 5–11 videos per individual.

## 2.4 | Video Analysis

High-speed videos were played back and used to quantify the 'capture type'. Three different behaviors were identified and used to describe the type of capture for each video recorded. These capture types were identified based on the displacement of anatomical landmarks, such as the eye and the shoulder (Figure 3A). No strict threshold was defined, as the two capture types were generally easy to distinguish: individuals either exhibited a clear forward propulsion (i.e. animals used ram feeding and compensatory suction) or showed little to no forward movement (i.e. animals remained static and used inertial suction). Videos in which the movement was ambiguous or intermediate were classified as *intermediate* (Figure 3A). The "ram" behavior involved the entire body accelerating towards the prey upon mouth opening, propelled by the anterior limbs and tail, corresponding more closely to a compensatory suction behavior (Figure 3A). The "static" behavior consisted of the animal being positioned just above the prey and opening its mouth rapidly without moving towards it, the prey then being sucked in by hyoid depression alone, corresponding to a pure inertial suction event (Figure 3A). The "intermediate" behavior mixed these two approaches: the individual was relatively close to the prey but still moved forward to reach it.

Next, videos were trimmed to start at the beginning of mouth opening and to end at the complete repositioning of the hyoid apparatus. The videos were converted to.mp4 format for use with DEEPLABCUT (Nath et al. 2019; Mathis et al. 2018). The frame rate and scale were identified for each video. In DEEPLABCUT, 50 frames were extracted per video, with seven markers manually placed on different body parts of the individual: the eye, the upper jaw tip, the lower jaw tip, the corner of the mouth, the ventral tip of the basibranchial (hyoid 1) and the ventral tip of the epibranchial (hyoid 2), and the shoulder (Figure 1B). The software used these manual annotations to train a convolutional neural network to detect points of interest, associating them with fixed structures in the images. Various image transformations and modifications were applied to enhance analysis throughout training. A total of 200 epochs were used to fully train the model that was then able to track the markers across all videos with human-like accuracy (0–5 pixels from exact target which is a negligible error; see Nath et al. 2019; Mathis et al. 2018). After using DLC to position the markers on each frame of the videos, each video was reviewed to check whether the markers were correctly placed on every frame. If the markers were accurate, the video and marker positions were saved. If not, the markers were corrected on the incorrect frames, and another DLC cycle was run. This process was repeated until the marker positions were accurate for every frame in each video. The likelihood was over 0.95 for all videos at the end of the training and marker placement in DLC. For each video, a.csv file was generated containing marker coordinates.

Data transformation and analysis were then performed using R with the "dplyr" and "tidyr" packages. Coordinates were transformed using the defined scale for each video to obtain values in cm for distance and velocity calculations. The marker position was smoothed using the "smooth.spline" function from R's base package to reduce artifacts while conserving biological data (Korff and McHenry 2011; Reinsch 1967; Skandalis et al. 2024; Wood 2017) and then calculate variables of interest. From the smoothed coordinates we calculated the gape

distance, the gape angle, the head angle (formed by the angle between the markers on the tip of the lower jaw, the eye, and the shoulder), and the hyoid depression distance at the level of the basibranchial (hyoid 1) and the epibranchial (hyoid 2) (Figure 1B). From the kinematic traces, we then extracted the maximum gape distance, maximum gape angle, maximum jaw opening and closing speed and acceleration, maximum head angle, maximum depression of the hyoid at both levels, the acceleration and speed of hyoid depression at both levels, the time to reach each maximum displacement, and finally the jaw and hyoid cycle duration. See Table S3 for raw values and Table 2 for means and standard deviations of the variables.

## 2.5 | Statistical Analyses

For both experiments, behavioral variables were transformed through a simple log transformation ($\log(x+1)$ to take into account zeros). We then assessed normality by examining the QQ-plot for each variable.

To test whether the choice of the first tunnel of the Y-maze was random, the observations were compared to a binomial distribution using a GLMER model with two parameters: light condition (light *vs.* dark) and population origin (surface vs. cave), with individual identity as a random effect. To compare the number of entries into the tunnels, Wilcoxon tests were used for each combination.

Chi-square ($\chi^2$) tests were performed to compare prey capture strategies. For normally distributed variables, we fitted a linear mixed-effects model with light condition, population of origin, and their interaction as fixed effects, and individual identity as a random effect. This was followed by a type II ANOVA when the interaction was non-significant, and a type III ANOVA when it was significant. For non-normal variables, we applied a rank transformation using the ART package in R, fitting the same model (origin and light condition as fixed effects, individual identity as a random effect), again followed by a type III ANOVA. Post-hoc tests with Bonferroni correction were then performed to identify which groups differed from one another. For all models,

**TABLE 2** | Means and standard deviations of the kinematic parameters extracted from the high-speed videos.

| Origin<br>Light condition | Surface<br>Light | Surface<br>Dark | Cave<br>Light | Cave<br>Dark |
|---|---|---|---|---|
| Maximal gape distance (cm) | 0.25 ± 0.07 | 0.22 ± 0.09 | 0.22 ± 0.07 | 0.19 ± 0.09 |
| Time to maximal gape distance (s) | 0.04 ± 0.01 | 0.04 ± 0.01 | 0.04 ± 0.01 | 0.04 ± 0.02 |
| Maximal gape angle (°) | 26.44 ± 10.00 | 23.28 ± 10.97 | 24.32 ± 8.75 | 20.59 ± 9.65 |
| Time to maximal gape angle (s) | 0.04 ± 0.01 | 0.05 ± 0.01 | 0.04 ± 0.01 | 0.04 ± 0.02 |
| Duration jaw cycle (s) | 0.10 ± 0.03 | 0.10 ± 0.02 | 0.08 ± 0.02 | 0.09 ± 0.04 |
| Maximum opening speed ($cm.s^{-1}$) | 11.49 ± 4.70 | 10.19 ± 4.12 | 11.87 ± 3.67 | 10.22 ± 4.07 |
| Maximum closing speed ($cm.s^{-1}$) | −12.29 ± 4.82 | −10.38 ± 4.17 | −11.60 ± 3.77 | −9.96 ± 5.05 |
| Maximum opening acceleration ($cm.s^{-2}$) | 1060.41 ± 719.5 | 1092.16 ± 726.06 | 1758.37 ± 1453.93 | 1299.71 ± 856.71 |
| Maximum closing acceleration ($cm.s^{-2}$) | 1139.16 ± 767.91 | 963.97 ± 547.96 | 1483.10 ± 1062.90 | 1153.99 ± 855.79 |
| Maximum head angle (°) | 152.17 ± 8.08 | 144.97 ± 13.52 | 150.99 ± 9.43 | 141.50 ± 11.69 |
| Time to maximal head angle (s) | 0.05 ± 0.04 | 0.16 ± 0.28 | 0.07 ± 0.15 | 0.16 ± 0.28 |
| Duration of hyoid 1 depression (s) | 0.02 ± 0.02 | 0.01 ± 0.02 | 0.01 ± 0.02 | 0.01 ± 0.02 |
| Maximal hyoid 1 depression (cm) | 0.37 ± 0.10 | 0.40 ± 0.11 | 0.41 ± 0.10 | 0.31 ± 0.11 |
| Time to maximal hyoid 1 depression (s) | 0.12 ± 0.09 | 0.12 ± 0.09 | 0.09 ± 0.05 | 0.12 ± 0.07 |
| Duration hyoid 1 cycle (s) | 0.87 ± 0.43 | 0.86 ± 0.42 | 0.67 ± 0.34 | 0.65 ± 0.32 |
| Maximal speed hyoid 1 depression ($cm.s^{-1}$) | 15.12 ± 5.08 | 14.93 ± 5.08 | 18.51 ± 6.04 | 12.22 ± 5.69 |
| Maximal speed hyoid 1 elevation ($cm.s^{-1}$) | −3.88 ± 2.12 | −4.26 ± 1.79 | −5.15 ± 2.75 | −4.05 ± 1.71 |
| Maximal acceleration hyoid1 depression ($cm.s^{-2}$) | 1570.94 ± 1092.03 | 1306.06 ± 691.02 | 2316.60 ± 1899.05 | 1423.39 ± 836.97 |
| Duration hyoid 2 depression (s) | 0.01 ± 0.02 | 0.01 ± 0.02 | 0.01 ± 0.02 | 0.01 ± 0.02 |
| Maximal hyoid 2 depression (cm) | 0.56 ± 0.10 | 0.45 ± 0.13 | 0.41 ± 0.14 | 0.36 ± 0.12 |
| Time to maximal hyoid 2 depression (s) | 0.09 ± 0.04 | 0.11 ± 0.06 | 0.09 ± 0.08 | 0.11 ± 0.10 |
| Duration hyoid 2 cycle (s) | 0.89 ± 0.40 | 0.85 ± 0.42 | 0.67 ± 0.37 | 0.62 ± 0.36 |
| Maximal speed hyoid 2 depression ($cm.s^{-1}$) | 19.77 ± 4.06 | 15.81 ± 4.79 | 17.02 ± 6.38 | 13.75 ± 6.05 |
| Maximal speed hyoid 2 elevation ($cm.s^{-1}$) | −4.60 ± 1.97 | −4.64 ± 1.89 | −5.35 ± 2.41 | −4.49 ± 2.31 |
| Maximal acceleration hyoid 2 depression ($cm.s^{-2}$) | 1577.70 ± 979.86 | 1338.27 ± 811.83 | 2110.83 ± 1662.31 | 1612.57 ± 1194.68 |

we report effect sizes to complement the p-values: partial eta-squared ($\eta^2_p$) for the main effects and the interaction, and a standardized effect size for each pairwise comparison. For non-normal variables (ART models), pairwise effect sizes are expressed on the rank scale.

## 3 | Results

### 3.1 | Olfactory and Exploratory Behaviors

The raw data are provided in Table S2, and the means ± standard deviations are reported in Table 1. Considering the total number of tunnel entries, salamanders entered the tunnel containing the food more frequently than the other tunnels (Figure 2A). Although animals appeared to make more tunnel entries under full-light conditions (Figure 2A), statistical analyses revealed no significant effect of either light condition or population of origin on the total number of tunnel entries (light condition: $F = 9.71$, $p = 0.089$; population: $F = 0.029$, $p = 0.88$).

The analysis of the first tunnel entered showed no significant difference from random choice under most experimental conditions (all $p > 0.05$), with correct first choices ranging from 52% to 62% (all $p > 0.05$ Figure 2B). The only exception was cave-dwelling individuals tested under full-light conditions, which entered the food-containing tunnel first significantly more often than expected by chance (33/50, 66%; $p = 0.03$; Figure 2B)

Overall, salamanders spent significantly more time in the food area (40.2% of the trial; Table S2; upper food quadrant + food tunnel; Figure 1A) than in the stone area (22.8%; Table S2; upper stone quadrant + stone tunnel; Figure 1A) or either of the two empty lower quadrants (18.5% each; Figure 2C; Table S2). No differences in the time spent in the food tunnel were detected between light conditions or populations. However, surface-dwelling individuals spent less time in the food tunnel under full-light conditions compared to total darkness (Figure 2D; Tables 1 and 3; $p = 0.04$).

The time spent in the stone area was significantly affected by light condition, with a strong interaction effect between light condition and population (Table 3). Under full-light conditions, salamanders spent more time in the stone section and stone tunnel (Table 1). Conversely, they spent less time in the empty sections under full light (Table 1). Finally, surface-dwelling salamanders entered their first tunnel more rapidly under full-light conditions (Tables 1 and 3; $p = 0.008$), whereas cave-dwelling individuals were the fastest to enter the correct tunnel containing the food in total darkness (Table 1).

### 3.2 | Type of Approach

The high-speed video analysis revealed different capture behaviors (Figure 3A) based on light conditions and the population of origin (surface-dwelling or cave-dwelling). The analysis shows a significantly higher proportion of "ram" behaviors in light conditions independent of the population origin ($\chi^2 = 50$; $p < 0.001$; Figure 3B). In contrast, more "static" captures (inertial suction) are observed under dark conditions ($\chi^2 = 21.28$; $p < 0.001$; Figure 3B). The "intermediate" type of approach showed no differences between the conditions ($\chi^2 = 1.09$; $p = 0.297$;Figure 3B).

### 3.3 | Feeding Kinematics

Raw kinematic data are provided in Table S3 and means ± standard deviations are provided in Table 2. Surface-dwelling and cave-dwelling individuals differed in gape distance and head angle with surface-dwelling individuals showing a greater gape distance and a greater head angle (Table 2). The distance and speed of hyoid 2 depression (epibranchial; Figure 1B) are also greater in surface-dwelling individuals (Table 2 and 4). Comparing surface-dwelling individuals under both light conditions, the head angle, and hyoid 2 depression metrics are higher under light conditions (Tables 2 and 4). When comparing surface-dwelling and cave-dwelling populations under light conditions, cave individuals show a faster mouth opening, higher hyoid 1 speeds, and a greater maximum hyoid 2 distance (Tables 2). In darkness, the hyoid 1 and 2 depression are more pronounced in surface-dwelling individuals (Table 2). Cave-dwelling individuals under light conditions displayed a greater head angle and an increased distance, speed, and acceleration of hyoid 1, as well as a greater hyoid 2 depression speed (Tables 2 and 4).

## 4 | Discussion

The aim of this study was to determine whether differences exist in the feeding behavior of individuals of *Calotriton asper* from cave-dwelling and surface-dwelling populations. Given the extreme conditions of cave environments, we hypothesized behavioral differences, particularly in prey detection, capture techniques, and feeding kinematics. Unexpectedly, no difference from random was observed for the first entry into a tunnel of the Y-maze, except for cave-dwelling individuals under light conditions showing a preference for the tunnel containing food (Figure 2B). However, regardless of the population origin or observation condition (light *vs.* darkness), individuals spent more time in the area with the food (Figure 2C) and entered the associated tunnel more frequently. This suggests that food detection might occur both in light and darkness through both olfactory and visual cues. The observation conditions significantly influenced the amount of time spent in the sector with a stone, with individuals observed under light conditions spending more time there (Tables 1 and 3). This pattern also applied to the frequency of tunnel entries (Figure 2A), likely due to the easier visual detection of tunnel entrances under light conditions, allowing for more exploration of the tunnel containing the stone.

In contrast, in darkness, surface-dwelling individuals seem to rely more on olfaction and spend more time in the sector and tunnel with food (Table 1 and 3). Previous research has shown that *Calotriton asper* relies primarily on vision for feeding (Uiblein et al. 1995), which could interfere with other senses. Thus, under light conditions, the surface-dwelling animals might focus more on vision and less on olfaction, possibly

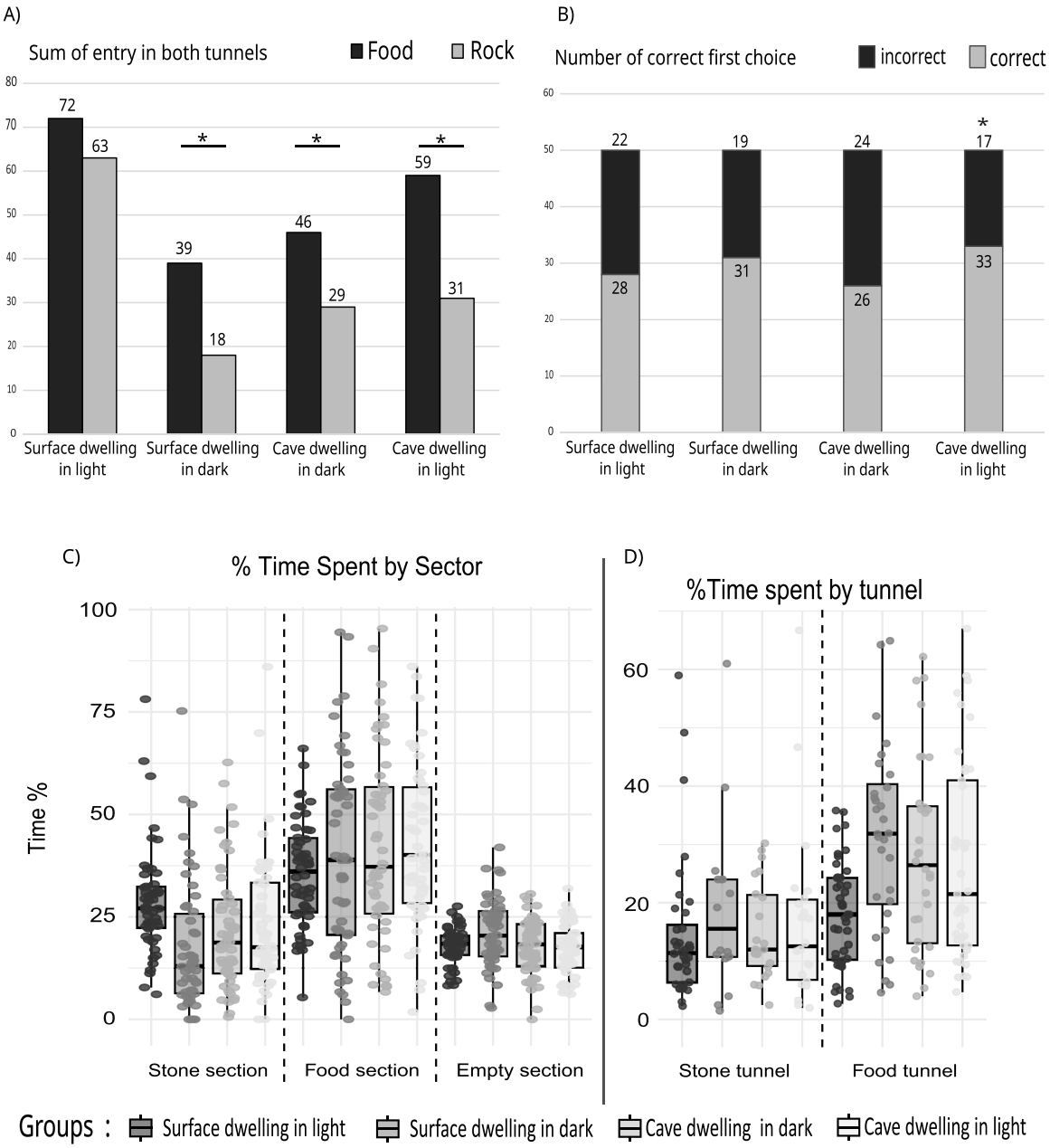


**FIGURE 2** | Results of Y-maze trials. (A) Reaction norm of the total number of entries into both tunnels of the maze based on observation conditions (light *vs.* dark) and population of origin. Sample size: $N = 10$ individuals, each tested 10 times in both conditions (total of 200 tests). Individuals were considered as random variables. (B) Reaction norm of the proportion of correct first entries into the tunnel containing food. The cave-dwelling animals in light conditions are the only ones to show a significant difference from random. Sample size: $N = 10$ individuals, each tested 10 times in both conditions (total of 200 tests). Individuals were considered as random variables. (C) boxplot of the percentage of time spent in the three sections of the maze, separated by observation conditions (light vs. dark). The Empty sector had twice the surface area (two quarters) of the food sector (one quarter) and the stone sector (one quarter). Therefore, to make the scale comparable, the raw data for the empty sector was divided by two before creating the boxplots. Sample size: $N = 10$ individuals, each tested 10 times in both conditions (total of 200 tests). D) boxplot of the percentage of time spent in one of two tunnels containing either food or a rock, by observation condition (light vs. darkness). Sample size: $N = 10$ individuals, each tested 10 times in both conditions (total of 200 tests).

explaining the reduced time spent near food, while in darkness, they might rely primarily on olfaction, which appears to enhance their focus on food. A study on snakes showed decreased performance under sensory conflict (Chen et al. 2012), but no such research has been conducted on salamanders. Surface-dwelling individuals under light conditions explored more, and spent less time in the food zone (Table 1). This exploratory behavior was greatly reduced in darkness where they stayed closer to the food once located (Table 1). Conversely, cave-dwelling individuals in light conditions appeared more exploratory than surface-dwelling individuals in the dark, entering and exiting tunnels more frequently (Figure 2A). This increased exploration in light conditions contrasts with other research which suggested that cave animals are more efficient at finding food in darkness. In cave environments, heightened exploratory behavior seems advantageous for locating scarce

**TABLE 3** | Results of the pairwise tests on the behavioral variables.

| Variables | Population of origin | Light condition | Interaction effect | Surface light versus dark | Cave light versus dark | Light cave versus surface | Dark cave versus surface | Surface light versus cave dark | Surface dark versuscave light |
|---|---|---|---|---|---|---|---|---|---|
| Time to first entry (s) | 0.905 ($\eta^2 = 0.00$) | 0.068 ($\eta^2 = 0.02$) | **0.008 ($\eta^2 = 0.04$)** | **< 0.001 (ES = 0.98)** | 1 (ES = 0.23) | 0.632 (ES = 0.40) | 0.861 (ES = 0.36) | 0.09 (ES = 0.62) | 0.13 (ES = 0.58) |
| Time to first correct entry (s) | 0.996 ($\eta^2 = 0.00$) | 0.255 ($\eta^2 = 0.01$) | 0.615 ($\eta^2 = 0.00$) | **0.003 (ES = 0.70)** | **0.034 (ES = 0.56)** | 1 (ES = 0.21) | 1 (ES = 0.07) | **0.004 (ES = 0.77)** | 0.133 (ES = 0.49) |
| Time in food sector (s) | 0.236 ($\eta^2 = 0.17$) | 0.84 ($\eta^2 = 0.00$) | 0.506 ($\eta^2 = 0.00$) | 1 (ES = 0.27) | 1 (ES = 0.08) | 1 (ES = 0.06) | 1 (ES = 0.12) | 1 (ES = 0.15) | 1 (ES = 0.21) |
| Time in food sector (%) | 0.236 ($\eta^2 = 0.17$) | 0.812 ($\eta^2 = 0.00$) | 0.497 ($\eta^2 = 0.00$) | 1 (ES = 0.24) | 1 (ES = 0.05) | 1 (ES = 0.10) | 1 (ES = 0.09) | 1 (ES = 0.15) | 1 (ES = 0.14) |
| Time in food tunnel (s) | 0.648 ($\eta^2 = 0.03$) | 0.566 ($\eta^2 = 0.00$) | 0.548 ($\eta^2 = 0.00$) | **0.04 (ES = 0.55)** | 0.361 (ES = 0.38) | 1 (ES = 0.20) | 1 (ES = 0.03) | 0.114 (ES = 0.57) | 0.800 (ES = 0.35) |
| Time in food tunnel (%) | 0.634 ($\eta^2 = 0.03$) | 0.610 ($\eta^2 = 0.00$) | 0.159 ($\eta^2 = 0.01$) | 0.094 (ES = 0.49) | 1 (ES = 0.09) | 1 (ES = 0.16) | 1 (ES = 0.24) | 1 (ES = 0.25) | 0.868 (ES = 0.33) |
| Time in stone sector (s) | 0.855 ($\eta^2 = 0.00$) | **< 0.001 ($\eta^2 = 0.07$)** | **0.001 ($\eta^2 = 0.05$)** | 0.627 (ES = 0.33) | **0.024 (ES = 0.58)** | 0.376 (ES = 0.50) | 0.732 (ES = 0.41) | 1 (ES = 0.08) | 1 (ES = 0.17) |
| Time in stone sector (%) | 0.966 ($\eta^2 = 0.00$) | **< 0.001 ($\eta^2 = 0.07$)** | **0.001 ($\eta^2$=0.05)** | 0.316 (ES = 0.39) | 0.067 (ES = 0.51) | 0.492 (ES = 0.47) | 0.627 (ES = 0.43) | 1 (ES = 0.04) | 1 (ES = 0.08) |
| Time in stone tunnel (s) | 0.281 ($\eta^2 = 0.14$) | **0.001 ($\eta^2 = 0.05$)** | **< 0.001 ($\eta^2 = 0.06$)** | 1 (ES = 0.10) | **< 0.001 (ES = 0.87)** | 0.967 (ES = 0.33) | 0.072 (ES = 0.63) | 0.178 (ES = 0.54) | 1 (ES = 0.24) |
| Time in stone tunnel (%) | 0.208 ($\eta^2 = 0.19$) | **0.001 ($\eta^2 = 0.05$)** | **< 0.001 ($\eta^2 = 0.06$)** | 1 (ES = 0.17) | **< 0.001 (ES = 0.79)** | 0.686 (ES = 0.37) | 0.089 (ES = 0.59) | 0.44 (ES = 0.42) | 1 (ES = 0.20) |
| Time in empty sector (%) | 0.202 ($\eta^2 = 0.19$) | **0.036 ($\eta^2 = 0.02$)** | 0.363 ($\eta^2 = 0.00$) | 0.751 (ES = 0.31) | 1 (ES = 0.05) | 1 (ES = 0.28) | 1 (ES = 0.02) | 1 (ES = 0.33) | 1 (ES = 0.03) |

*Note:* Table entries are p-values, followed in parentheses by the effect size: partial eta-squared ($\eta^2_p$) for the main effects and interaction, and the standardized effect size (ES) from the ART model for the pairwise post-hoc comparisons. Pairwise p-values are ART contrasts with Bonferroni adjustment. Bold values indicate significant differences ($p < 0.05$)

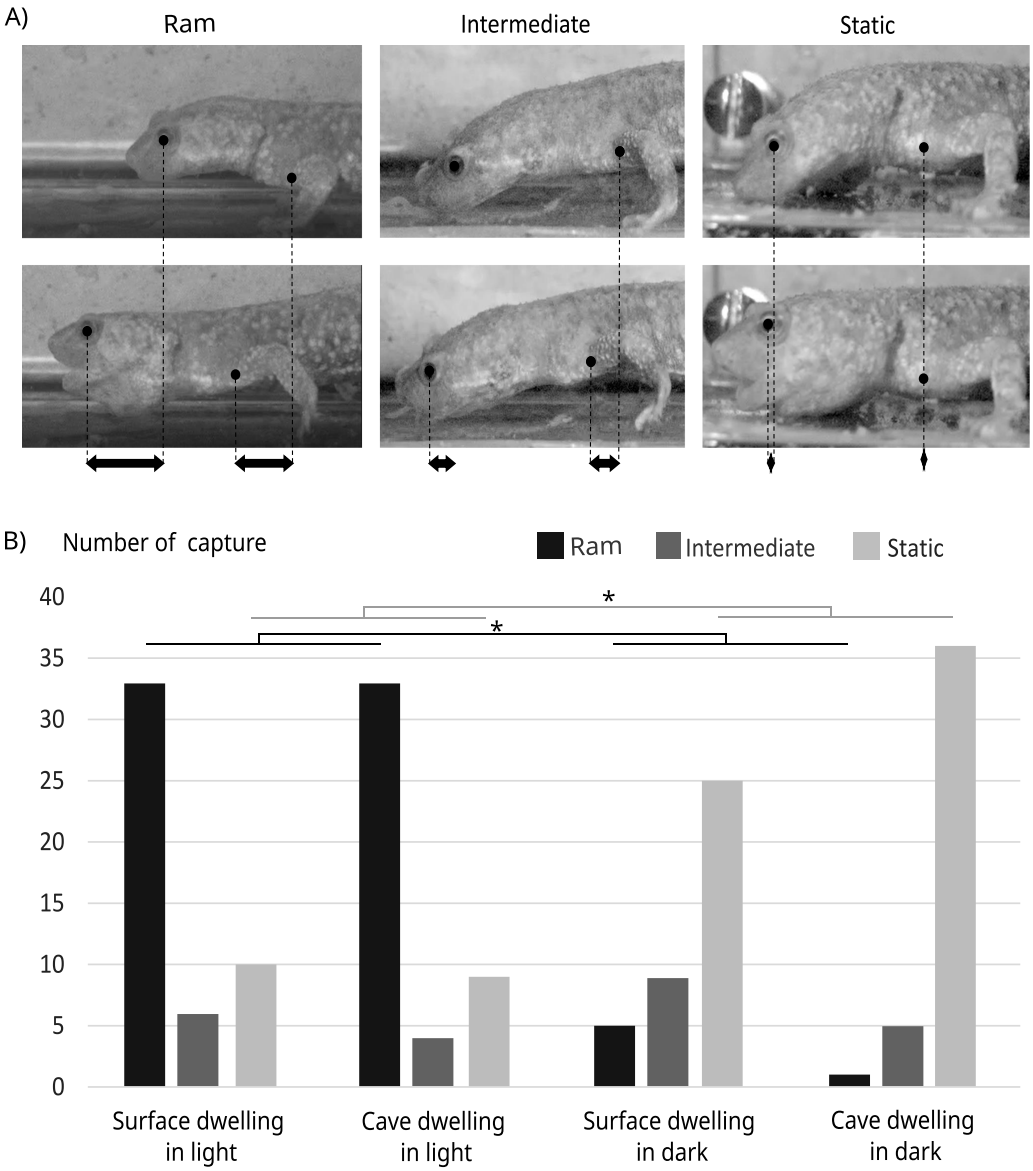


**FIGURE 3** | prey capture types. (A) Images taken from high-speed videos at the start of prey capture and at peak gape. Three types of behaviors are observed (ram, intermediate, and static). The differences between these conditions are noticeable by the position of the eyes and shoulders between the time points represented by the images. (B) Reaction norm showing the number of captures by type based on experimental light condition and the origin of the population.

food sources which may explain the results observed here (Manenti and Ficetola 2013; Manenti et al. 2013). In summary, as expected, a preference for the food zone was detected (Figure 2; Table 1), but no significant differences were observed between populations. The observed differences were instead tied to environmental conditions, indicating plasticity in exploratory behavior and sensory cues used in both cave-dwelling and surface-dwelling populations. This behavioral flexibility could enhance adaptation to different environments, facilitating the colonization of caves by *Calotriton asper* (Crispo 2008).

Concerning prey capture, differences emerged between population origin and lighting conditions. The capture technique differed strongly based on lighting conditions. In the light, individuals, irrespective of the population, could see their target and adopted a more ram-like strategy (Figure 3). During this behavior, animals maintain a greater distance, move rapidly towards the prey, and open their mouth later to perform compensatory suction. In contrast, in the dark, vision could not be used and prey capture relied on other senses. Here, animals positioned themselves closer to the prey, with a lower head angle, and performed mostly inertial suction to capture prey directly in front of their mouths (Figure 3). Moreover, by positioning their mouths close to the surface, they likely took advantage of wall effects which have been shown to improve suction performance (Nauwelaerts et al. 2007). These changes, including the head angle (Table 2 and 4), were significantly different in light versus darkness. Importantly, this shift in capture style was independent of the population of origin (Figure 3). This demonstrates behavioral plasticity in both groups, with the species capable of employing both suction types depending on the situation (Van Damme and Aerts 1997). This plasticity underscores again the advantage of this species in colonizing new environments.

**TABLE 4** | Results of the pairwise tests on the kinematic variables.

| Variables | Population Of origin | Light condition | Interaction effect | Surface light versus dark | Cave light versus dark | Light cave versus surface | Dark Cave versus Surface | Surface light vs Cave dark | Surface dark vs Cave light |
|---|---|---|---|---|---|---|---|---|---|
| Maximal gape distance (cm) | 0.151 ($\eta^2 = 0.12$) | 0.076 ($\eta^2 = 0.16$) | 0.796 ($\eta^2 = 0.00$) | 1 (ES = 0.37) | 1 (ES = 0.49) | 1 (ES = 0.29) | 1 (ES = 0.41) | 0.226 (ES = 0.78) | 1 (ES = 0.08) |
| Time to maximal gape distance | **0.021 ($\eta^2 = 0.29$)** | 0.813 ($\eta^2 = 0.00$) | 0.604 ($\eta^2 = 0.02$) | 1 (ES = 0.11) | 1 (ES = 0.08) | 1 (ES = 0.04) | 1 (ES = 0.15) | 1 (ES = 0.04) | 1 (ES = 0.07) |
| Maximal gape angle (°) | 0.341 ($\eta^2 = 0.06$) | 0.154 ($\eta^2 = 0.12$) | 0.918 ($\eta^2 = 0.00$) | 1 (ES = 0.06) | 1 (ES = 0.13) | 1 (ES = 0.01) | 1 (ES = 0.05) | 1 (ES = 0.11) | 1 (ES = 0.08) |
| Time to maximal gape angle | **0.042 ($\eta^2 = 0.24$)** | 0.643 ($\eta^2 = 0.01$) | 0.979 ($\eta^2 = 0.00$) | 1 (ES = 0.01) | 1 (ES = 0.02) | 1 (ES = 0.07) | 1 (ES = 0.08) | 1 (ES = 0.10) | 1 (ES = 0.06) |
| Duration jaw cycle | **0.037 ($\eta^2 = 0.25$)** | 0.5 ($\eta^2 = 0.03$) | 0.568 ($\eta^2 = 0.02$) | 1 (ES = 0.04) | 1 (ES = 0.17) | 1 (ES = 0.04) | 1 (ES = 0.17) | 1 (ES = 0.12) | 1 (ES = 0.00) |
| Maximum opening speed | 0.699 ($\eta^2 = 0.02$) | 0.093 ($\eta^2 = 0.11$) | 0.924 ($\eta^2 = 0.00$) | 1 (ES = 0.03) | 1 (ES = 0.01) | 1 (ES = 0.13) | 1 (ES = 0.09) | 1 (ES = 0.12) | 1 (ES = 0.10) |
| Maximum closing speed | 0.666 ($\eta^2 = 0.01$) | 0.069 ($\eta^2 = 0.17$) | 0.898 ($\eta^2 = 0.00$) | 1 (ES = 0.49) | 1 (ES = 0.56) | 1 (ES = 0.09) | 1 (ES = 0.16) | 0.800 (ES = 0.65) | 1 (ES = 0.40) |
| Max opening acceleration ($cms^{-2}$) | **0.019 ($\eta^2 = 0.24$)** | 0.311 ($\eta^2 = 0.06$) | 0.341 ($\eta^2 = 0.05$) | 1 (ES = 0.01) | 1 (ES = 0.38) | 0.205 (ES = 0.63) | 1 (ES = 0.26) | 1 (ES = 0.25) | 0.224 (ES = 0.64) |
| Maximum closing acceleration | 0.220 ($\eta^2 = 0.08$) | 0.205 ($\eta^2 = 0.09$) | 0.770 ($\eta^2 = 0.01$) | 1 (ES = 0.23) | 1 (ES = 0.37) | 1 (ES = 0.36) | 1 (ES = 0.22) | 1 (ES = 0.01) | 0.628 (ES = 0.59) |
| Max head angle (°) | 0.226 ($\eta^2 = 0.09$) | **0.010 ($\eta^2 = 0.34$)** | 0.581 ($\eta^2 = 0.02$) | 1 (ES = 0.40) | 1 (ES = 0.07) | 1 (ES = 0.14) | 1 (ES = 0.19) | 1 (ES = 0.20) | 1 (ES = 0.26) |
| Maximal hyoid 1 depression (cm) | **0.006 ($\eta^2 = 0.05$)** | **0.002 ($\eta^2 = 0.11$)** | **0.003 ($\eta^2 = 0.35$)** | 1 (ES = 0.41) | **0.046 (ES = 1.16)** | 1 (ES = 0.53) | 0.092 (ES = 1.04) | 0.683 (ES = 0.63) | 1 (ES = 0.11) |
| Time to maximal hyoid 1 depression | 0.394 ($\eta^2 = 0.05$) | 0.510 ($\eta^2 = 0.03$) | 0.346 ($\eta^2 = 0.06$) | 1 (ES = 0.41) | 1 (ES = 0.02) | 1 (ES = 0.12) | 0.634 (ES = 0.55) | 1 (ES = 0.14) | 0.701 (ES = 0.52) |
| Duration hyoid 1 cycle | 0.068 ($\eta^2 = 0.19$) | 0.976 ($\eta^2 = 0.00$) | 0.900 ($\eta^2 = 0.00$) | 1 (ES = 0.10) | 1 (ES = 0.02) | 1 (ES = 0.01) | 1 (ES = 0.09) | 1 (ES = 0.01) | 1 (ES = 0.11) |
| Maximal hyoid 1 depression speed ($cms^{-1}$) | 0.067 ($\eta^2 = 0.00$) | **< 0.001 ($\eta^2 = 0.32$)** | **0.008 ($\eta^2 = 0.30$)** | 1 (ES = 0.02) | **0.010 (ES = 1.37)** | 0.459 (ES = 0.68) | 0.533 (ES = 0.67) | 0.436 (ES = 0.69) | 0.443 (ES = 0.70) |
| Maximal speed hyoid 1 elevation | 0.214 ($\eta^2 = 0.08$) | 0.630 ($\eta^2 = 0.01$) | **0.047 ($\eta^2 = 0.19$)** | 1 (ES = 0.27) | 0.625 (ES = 0.44) | 0.239 (ES = 0.56) | 1 (ES = 0.15) | 1 (ES = 0.11) | 1 (ES = 0.29) |
| Maximal hyoid 1 depression acceleration ($cms^{-2}$) | 0.090 ($\eta^2 = 0.14$) | **0.017 ($\eta^2 = 0.26$)** | 0.252 ($\eta^2 = 0.07$) | 1 (ES = 0.27) | 0.150 (ES = 0.75) | 0.380 (ES = 0.59) | 1 (ES = 0.11) | 1 (ES = 0.16) | 0.078 (ES = 0.86) |

(Continues)

**TABLE 4** | (Continued)

| Variables | Population Of origin | Light condition | Interaction effect | Surface light versus dark | Cave light versus dark | Light cave versus surface | Dark Cave versus Surface | Surface light vs Cave dark | Surface dark vs Cave light |
|---|---|---|---|---|---|---|---|---|---|
| Maximal hyoid 2 depression (cm) | **< 0.001 ($\eta^2 = 0.63$)** | **< 0.001 ($\eta^2 = 0.44$)** | 0.198 ($\eta^2 = 0.09$) | **0.022 (ES = 0.93)** | 0.769 (ES = 0.44) | **0.002 (ES = 1.23)** | 0.110 (ES = 0.73) | **< 0.001 (ES = 1.66)** | 1 (ES = 0.30) |
| Time to maximal hyoid 2 depression | 0.457 ($\eta^2 = 0.04$) | 0.322 ($\eta^2 = 0.06$) | 0.705 ($\eta^2 = 0.01$) | 1 (ES = 0.44) | 1 (ES = 0.27) | 1 (ES = 0.11) | 1 (ES = 0.05) | 1 (ES = 0.38) | 1 (ES = 0.33) |
| Duration hyoid 2 cycle | **0.029 ($\eta^2 = 0.26$)** | 0.699 ($\eta^2 = 0.01$) | 0.927 ($\eta^2 = 0.00$) | 1 (ES = 0.07) | 1 (ES = 0.02) | 1 (ES = 0.02) | 1 (ES = 0.07) | 1 (ES = 0.00) | 1 (ES = 0.09) |
| Maximal hyoid 2 depression speed ($cms^{-1}$) | **0.002 ($\eta^2 = 0.38$)** | **< 0.001 ($\eta^2 = 0.51$)** | 0.857 ($\eta^2 = 0.00$) | **0.048 (ES = 0.74)** | 0.082 (ES = 0.68) | 0.194 (ES = 0.55) | 0.415 (ES = 0.49) | **< 0.001 (ES = 1.23)** | 1 (ES = 0.18) |
| Maximal speed hyoid 2 elevation | 0.191 ($\eta^2 = 0.09$) | 0.148 ($\eta^2 = 0.11$) | 0.091 ($\eta^2 = 0.15$) | 1 (ES = 0.04) | 0.262 (ES = 0.48) | 0.323 (ES = 0.43) | 1 (ES = 0.08) | 1 (ES = 0.04) | 0.541 (ES = 0.40) |
| Maximal acceleration hyoid 2 depression | 0.150 ($\eta^2 = 0.11$) | 0.078 ($\eta^2 = 0.16$) | 0.737 ($\eta^2 = 0.01$) | 1 (ES = 0.24) | 0.979 (ES = 0.36) | 1 (ES = 0.30) | 1 (ES = 0.18) | 1 (ES = 0.06) | 0.263 (ES = 0.54) |

*Note:* Table entries are *p* values, each followed in parentheses by its effect size: partial eta-squared ($\eta^2_p$) for the main effects and interaction, and the standardized effect size (ES) from the model for the pairwise comparisons. Pairwise p-values are Bonferroni-corrected. Non-normal variables are underlined. Bolded values highlight significant differences.

While different capture techniques exist between surface-dwelling and cave populations in other species such as *Astyanax mexicanus*, these are generally rooted in more profound genetic and anatomical differences (Gallman et al. 2020; Yoshizawa et al. 2010). It is rare for an individual to exhibit both techniques and show flexibility based on light conditions. The two morphotypes of *Astyanax mexicanus* show pronounced morphological differences, including eye loss, depigmentation, and other traits adapted to cave life, which are not present in the *Calotriton* populations of the Pyrenees. The divergence between *Astyanax* morphotypes occurred relatively recently (< 30,000 years; Fumey et al. 2018), while the formation of different *Calotriton* lineages in the Pyrenees dates to the Last Glacial Maximum (20 000 to 14 000 years ago; Lucati et al. 2020). Although limited gene flow occurs between populations today (Valbuena-Ureña et al. 2018) Their relatively recent differentiation compared with that of *Astyanax*, suggests that certain typical cave-dwelling traits may not yet have evolved.

Finally, comparisons between surface and cave-dwelling individuals under their natural lighting conditions showed the most differences in prey capture kinematics. Surface-dwelling individuals seem to exhibit more exaggerated movements, including a wider mouth opening and greater hyoid depression (Table 2). However, although surface-dwelling individuals were able to adapt their capture style to darkness, some differences remained between populations. For example, although surface-dwelling individuals in darkness depressed their hyoid less and more slowly compared when they fed in light (Table 2), they still showed more movement than cave-dwelling individuals (Figure 3B). This suggests that in darkness cave-dwelling individuals may be more efficient and may take greater advantage of wall-effects. Similarly, cave-dwelling individuals in light opened their mouths faster and deployed their hyoid apparatus more forcefully than surface-dwelling individuals under the same conditions (Table 2). Therefore, it seems that when individuals experience environmental shifts, they tend to overcompensate in their movements, potentially leading to a less efficient capture. It would be interesting to explore whether the differences observed between surface and cave-dwelling populations diminish over time when kept in dark or light conditions, respectively suggesting acclimatization to light conditions.

Despite these insights, several limitations must be acknowledged. First, the lack of directly comparable model systems is limiting our ability to contextualize these results broadly. Second, the experiments were conducted under controlled conditions, which do not fully replicate the ecological dynamics in natural cave systems. Third, small sample sizes and population variability may influence the interpretation of the observed patterns and future work should be done including more individuals. Moreover, testing whether individuals change behaviors over time when kept under different light conditions would be insightful.

## 5 | Conclusion

We observed significant differences in the capture style depending on the light conditions with both populations showing flexibility. Exploratory behavior was overall rather similar between populations and was influenced by light

conditions, with animals in darkness exhibiting less exploration and staying closer to food sources. Cave-dwelling individuals did not detect prey faster, contrary to our expectations. Detailed analyses of feeding kinematics revealed differences in the mouth opening angle and movement of the hyoid apparatus, with higher speeds and accelerations under light conditions. Although some of these differences result from changes in capture style, individuals in environments different from their natural habitat did not exhibit the same kinematics. In conclusion, while the two populations of *Calotriton asper* differ in their capture styles, they both display a high degree of behavioral plasticity. Subtle adaptive differences may provide advantages in their respective habitats, but both populations can adapt to variable light conditions.


### Acknowledgments

The authors would like to thank the staff at the SETE station for their hospitality. This research was funded by a European Research Council Starting Grant (SERI-funded grant M822.00039) to A.-C.F. Open access publication funding provided by COUPERIN CY26.


### Conflicts of Interest

The authors declare no conflicts of interest.

### Data Availability Statement

The data that supports the findings of this study are available in the supplementary material of this article. The scripts used for statistical analysis and figures are publicly available on GitHub: https://github.com/Noaheier/Influence-of-habitat-use-on-prey-capture-behavior-and-kinematics-in-the-Pyrenean-brook-newt-.git.

### References


Borghuis, B. G., and A. Leonardo. 2015. "The Role of Motion Extrapolation in Amphibian Prey Capture." *Journal of neuroscience* 35: 15430–15441.

Cartwright, R. A., R. S. Schwartz, A. L. Merry, and M. M. Howell. 2017. "The Importance of Selection in the Evolution of Blindness in Cavefish." *BMC Evolutionary Biology* 17: 45.

Castilla, A. M., R. Richer, A. Herrel, A. A. T. Conkey, J. Tribuna, and M. Al-Thani. 2011. "First Evidence of Scavenging Behaviour in the Herbivorous Lizard *Uromastyx aegyptia microlepis*." *Journal of Arid Environments* 75: 671–673.

Chen, Q., H. Deng, S. E. Brauth, L. Ding, and Y. Tang. 2012. "Reduced Performance of Prey Targeting in Pit Vipers With Contralaterally Occluded Infrared and Visual Senses." *PLoS One* 7: e34989.

Crispo, E. 2008. "Modifying Effects of Phenotypic Plasticity on Interactions Among Natural Selection, Adaptation and Gene Flow." *Journal of Evolutionary Biology* 21: 1460–1469.

Culver, D. C., and T. Pipan. 2009. "The Biology of Caves and Other Subterranean Habitats." *Integrative and Comparative Biology* 49: 473–474.

Van Damme, J., and P. Aerts. 1997. "Kinematics and Functional Morphology of Aquatic Feeding in Australian Snake-Necked Turtles (Pleurodira; *Chelodina*)." *Journal of Morphology* 233: 113–125.

Day, S. W., T. E. Higham, A. Y. Cheer, and P. C. Wainwright. 2005. "Spatial and Temporal Patterns of Water Flow Generated by Suction-Feeding Bluegill Sunfish *Lepomis macrochirus* Resolved by Particle Image Velocimetry." *Journal of Experimental Biology* 208: 2661–2671.

Deban, S. M. 2003. "Constraint and Convergence in the Evolution of Salamander Feeding." In *Vertebrate Biomechanics and Evolution*, edited by V. L. Bels, J.-P. Gasc, and A. Casinos. BIOS Scienctific publishers.

Dumas, P., and B. Chris. 1998. "The Olfaction in *Proteus anguinus*: A Behavioural and Cytological Study." *Behavioural Processes* 43: 107–113.

Fumey, J., H. Hinaux, C. Noirot, C. Thermes, S. Rétaux, and D. Casane. 2018. "Evidence for Late Pleistocene Origin of *Astyanax mexicanus* Cavefish." *BMC Evolutionary Biology* 18: 43.

Gallman, K., E. Fortune, D. Rivera, and D. Soares. 2020. "Differences in Behavior Between Surface and Cave *Astyanax mexicanus* May Be Mediated by Changes in Catecholamine Signaling." *Journal of Comparative Neurology* 528: 2639–2653.

Gibert, J., and L. Deharveng. 2002. "Subterranean Ecosystems: A Truncated Functional Biodiversity: This Article Emphasizes the Truncated Nature of Subterranean Biodiversity at Both the Bottom (No Primary Producers) and the Top (Very Few Strict Predators) of Food Webs and Discusses the Implications of This Truncation Both From Functional and Evolutionary Perspectives." *Bioscience* 52: 473–481.

Grant, P. R., and B. R. Grant. 2005. "Darwin's Finches." *Current Biology* 15: R614–R615.

Guillaume, O., M. Deluen, A. Raffard, O. Calvez, and A. Trochet. 2020. "Reduction in the Metabolic Levels Due to Phenotypic Plasticity in the Pyrenean Newt, *Calotriton asper*, During Cave Colonization." *Ecology and Evolution* 10: 12983–12989.

Herrel, A., K. Huyghe, B. Vanhooydonck, et al. 2008. "Rapid Large Scale Evolutionary Divergence in Morphology and Performance Associated With Exploitation of a Different Dietary Resource." *Proceedings of the National Academy of Sciences* 105: 4792–4795.

Herrel, A., J. C. O'Reilly, A.-C. Fabre, C. Bardua, R. Boistel, and S. Gorb. 2019. "Feeding in Amphibians: Evolutionary Transformations and Phenotypic Diversity as Drivers of Feeding System Diversity." In *Feeding in Vertebrates: Evolution, Morphology, Behavior, Biomechanics*, edited by V. L. Bels and I. Q. Wishaw, 431–467. Springer Verlag.

Herrel, A., J. Podos, S. K. Huber, and A. P. Hendry. 2005a. "Bite Performance and Morphology in a Population of Darwin's Finches: Implications for the Evolution of Beak Shape." *Functional Ecology* 19: 43–48.

Herrel, A., J. Podos, S. K. Huber, and A. P. Hendry. 2005b. "Evolution of Bite Force in Darwin's Finches: A Key Role for Head Width." *Journal of Evolutionary Biology* 18: 669–675.

Hervant, F., J. Mathieu, and J. P. Durand. 2000. "Metabolism and Circadian Rhythms of the European Blind Cave Salamander *Proteus anguinus* and a Facultative Cave Dweller, the Pyrenean Newt (*Euproctus asper*)." *Canadian Journal of Zoology* 78: 1427–1432.

Hervant, F., J. Mathieu, and J. Durand. 2001. "Behavioural, Physiological, and Metabolic Responses to Long-Term Starvation and Refeeding in a Blind Cave-Dwelling (*Proteus anguinus*) and a Surface-Dwelling (*Euproctus asper*) Salamander." *Journal of Experimental Biology* 204: 269–281.

Issartel, J., Y. Voituron, O. Guillaume, J. Clobert, and F. Hervant. 2010. "Selection of Physiological and Metabolic Adaptations to Food Deprivation in the Pyrenean Newt Calotriton Asper During Cave Colonisation." *Comparative Biochemistry and Physiology. Part A, Molecular & Integrative Physiology* 155, no. 1: 77–83.

Korff, W. L., and M. J. McHenry. 2011. "Environmental Differences in Substrate Mechanics Do Not Affect Sprinting Performance in Sand Lizards (*Uma scoparia* and *Callisaurus draconoides*)." *Journal of Experimental Biology* 214, no. 1: 122–130.

Larsen, J. H., and D. J. Guthrie. 1975. "The Feeding System of Terrestrial Tiger Salamanders (*Ambystoma tigrinum melanostictum* Baird)." *Journal of Morphology* 147: 137–153.

Lauder, G. V., and H. B. Shaffer. 1986. "Functional Design of the Feeding Mechanism in Lower Vertebrates: Unidirectional and

Bidirectional Flow Systems in the Tiger Salamander." *Zoological Journal of the Linnean Society* 88: 277–290.

Lucati, F., M. Poignet, A. Miró, et al. 2020. "Multiple Glacial Refugia and Contemporary Dispersal Shape the Genetic Structure of an Endemic Amphibian From the Pyrenees." *Molecular Ecology* 29: 2904–2921.

Manenti, R., M. Denoël, and G. F. Ficetola. 2013. "Foraging Plasticity Favours Adaptation to New Habitats in Fire Salamanders." *Animal Behaviour* 86: 375–382.

Manenti, R., and G. F. Ficetola. 2013. "Salamanders Breeding in Subterranean Habitats: Local Adaptations or Behavioural Plasticity?" *Journal of Zoology* 289: 182–188.

Manenti, R., E. Lunghi, B. Barzaghi, A. Melotto, M. Falaschi, and G. F. Ficetola. 2020. "Do Salamanders Limit the Abundance of Groundwater Invertebrates in Subterranean Habitats?" *Diversity* 12: 161.

Mathis, A., P. Mamidanna, K. M. Cury, et al. 2018. "Deeplabcut: Markerless Pose Estimation of User-Defined Body Parts With Deep Learning." *Nature Neuroscience* 21: 1281–1289.

Moran, D., R. Softley, and E. J. Warrant. 2014. "Eyeless Mexican Cavefish Save Energy by Eliminating the Circadian Rhythm in Metabolism." *PLoS One* 9: e107877.

Nath, T., A. Mathis, A. C. Chen, A. Patel, M. Bethge, and M. W. Mathis. 2019. "Using Deeplabcut for 3D Markerless Pose Estimation Across Species and Behaviors." *Nature Protocols* 14: 2152–2176.

Nauwelaerts, S., C. Wilga, C. Sanford, and G. Lauder. 2007. "Hydrodynamics of Prey Capture in Sharks: Effects of Substrate." *Journal of the Royal Society Interface* 4: 341–345.

Phillips, J. G., D. B. Fenolio, S. L. Emel, and R. M. Bonett. 2017. "Hydrologic and Geologic History of the Ozark Plateau Drive Phylogenomic Patterns in a Cave-Obligate Salamander." *Journal of Biogeography* 44: 2463–2474.

Poulson, T. L., and W. B. White. 1969. "The Cave Environment." *Science* 165: 971–981.

Reinsch, C. H. 1967. "Smoothing by Spline Functions." *Numerische Mathematik* 10: 177–183.

Sánchez-Hernández, J., A. Montori, and G. A. Llorente. 2019. "Ontogenetic Dietary Shifts and Food Resource Partitioning in a Stream-Dwelling Urodela Community: Mechanisms to Allow Coexistence Across Seasons." *Russian Journal of Herpetology* 26: 135–149.

Schwenk, K. 2000. *Feeding. Form, Function, And Evolution in Tetrapod Vertebrates*, 537. Academic Press.

Skandalis, D. A., V. B. Baliga, B. Goller, and D. L. Altshuler. 2024. "The Spatiotemporal Richness of Hummingbird Wing Deformations." *Journal of Experimental Biology* 227, no. 10: jeb246223.

Soares, D., and M. L. Niemiller. 2020. "Extreme Adaptation in Caves." *Anatomical Record* 303: 15–23.

Soons, J., A. Genbrugge, J. Podos, et al. 2015. "Is Beak Morphology in Darwin's Finches Tuned to Loading Demands?" *PLoS One* 10: e0129479.

Soons, J., A. Herrel, A. Genbrugge, et al. 2010. "Mechanical Stress, Fracture Risk and Beak Evolution in Darwin's Ground Finches (Geospiza)." *Philosophical Transactions of the Royal Society, B: Biological Sciences* 365: 1093–1098.

Talavera, A., M. Palmada-Flores, B. Burriel-Carranza, et al. 2024. "Genomic Insights into the Montseny Brook Newt (*Calotriton arnoldi*), a Critically Endangered Glacial Relict." *iScience* 27: 108665.

Uiblein, F., J. P. Durand, C. Juberthie, and J. Parzefall. 1992. "Predation in Caves: The Effects of Prey Immobility and Darkness on the Foraging Behaviour of Two Salamanders, *Euproctus asper* and *Proteus anguinus*." *Behavioural Processes* 28: 33–40.

Uiblein, F., S. Engelke, and J. Parzefall. 1995. "Trade-Off Between Visual Detectability and Nutrient Content in the Patch Choice of the Pyrenean Salamander *Euproctus asper*." *Ethology* 101: 39–45.

Valbuena-Ureña, E., N. Oromi, A. Soler-Membrives, et al. 2018. "Jailed in the Mountains: Genetic Diversity and Structure of an Endemic Newt Species Across the Pyrenees." *PLoS One* 13: e0200214.

Venarsky, M. P., and B. M. Huntsman. 2018. "Food Webs in Caves." In *Cave Ecology. Ecological Studies* (235). Springer Verlag.

Voituron, Y., M. De Fraipont, J. Issartel, O. Guillaume, and J. Clobert. 2010. "Extreme Lifespan of the Human Fish (*Proteus anguinus*): A Challenge for Ageing Mechanisms." *Biology Letters* 7: 105–107.

Wood, S. N. 2017. *Generalized Additive Models: An Introduction With R* (2nd ed. CRC Press.

Yoshizawa, M., Š. Gorički, D. Soares, and W. R. Jeffery. 2010. "Evolution of a Behavioral Shift Mediated by Superficial Neuromasts Helps Cavefish Find Food in Darkness." *Current Biology* 20: 1631–1636.

## Supporting Information

Additional supporting information can be found online in the Supporting Information section.

**Supporting File 1:** jez70131-sup-0001-Supplementary_Table_1.pdf.
**Supporting File 2:** jez70131-sup-0002-Supplementary_Table_2.xlsx.
**Supporting File 3:** jez70131-sup-0003-Supplementary_Table_3.xlsx.